Radiation Hydrodynamical Simulations of Cepheids.

Friedrich Kupka

jointly with

Eva Mundprecht, Herbert Muthsam

Faculty of Mathematics

University of Vienna, Austria

Outline

- Contributors, Collaborators
- Motivation
- The ANTARES Code
- The Numerical Challenges
- Simulation Results
- Recent Work and Outlook

ANTARES - Contributors and Collaborators

Bernhard Löw-Baselli, Hannes Grimm-Strele, Natalie Happenhofer, Peter Schiansky

Faculty of Mathematics, University of Vienna, Austria

Florian Zaussinger

LAS, BTU Cottbus, Germany

Jérôme Ballot

Laboratoire d'Astrophysique, Obs. de Midi-Pyréenées, Toulouse, France

Michael M. Montgomery, Kevin Luecke

Department of Astronomy, Univ. of Austin, Texas, USA

Othmar Koch[1,2]

[1]formerly at Faculty of Mathematics, University of Vienna, Austria
[2]now at ASC, Vienna University of Technology, Austria

ANTARES - Contributors and Collaborators

Arno Mayrhofer[3,4], Christof Obertscheider[3,5]

[3]formerly at Faculty of Mathematics, University of Vienna, Austria
[4]now at Univ. of Manchester, UK; [5]now at Magna International Inc.

Mathias Langer[6], Patrick Lenz[7]

[6]formerly at Faculty of Mathematics, University of Vienna, Austria
[7]now at Institute of Astronomy, University of Vienna, Austria

---

Inmaculada Higueras

Universidad Pública de Navarra, Pamplona, Spain

Hendrik C. Spruit

MPI for Astrophysics, Garching, Germany

Marie-Jo Goupil, Kévin Belkacem, Réza Samadi

LESIA, Obs. de Paris, Section de Meudon, France

Motivation I

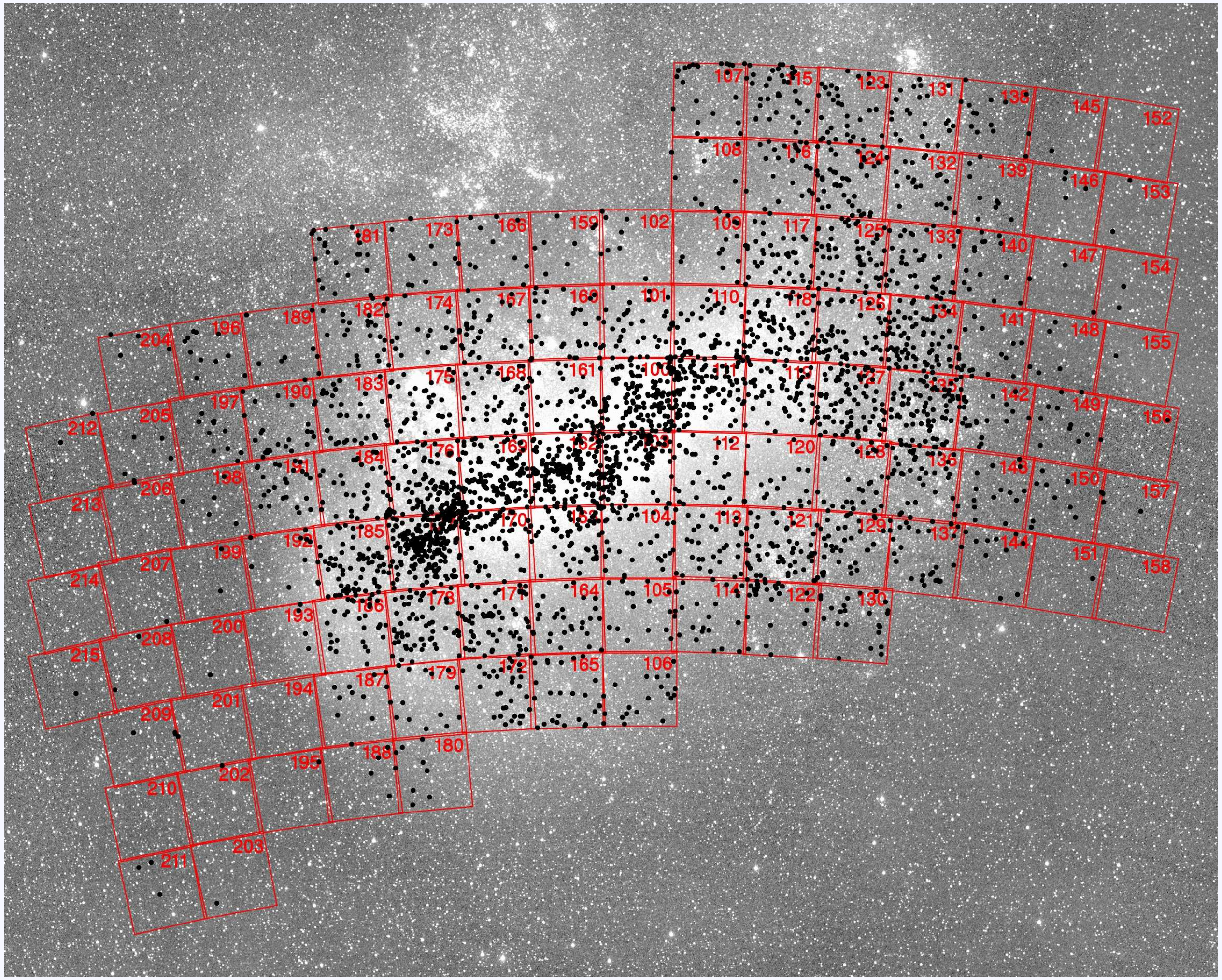

Fig. 4. OGLE-III fields in the LMC. Dots indicate positions of classical Cepheids from the OIII-CVS catalog. The background image of the LMC is originated from the ASAS wide field sky survey.

Cepheids in the OGLE-III field of the LMC (Soszyński et al. 2008, Acta Astron. 58, 163).

Motivation II

Astrophysical interest

- Cepheids are an important part of the cosmic distance ladder
- discrepancies have been found when comparing masses from stellar evolution and stellar pulsation modelling
- double-mode pulsators (even triple-mode) are observed
- period ratios sensitive to metallicity Z
- recently, even non-radial modes have been clearly identified in classical pulsators (RR Lyr)
- 1D models yield mixed results about their location in the HRD
- interpretation of the relations of period P, luminosity L, colour, and metallicity Z: can we trust 1D models ?!?

Motivation III

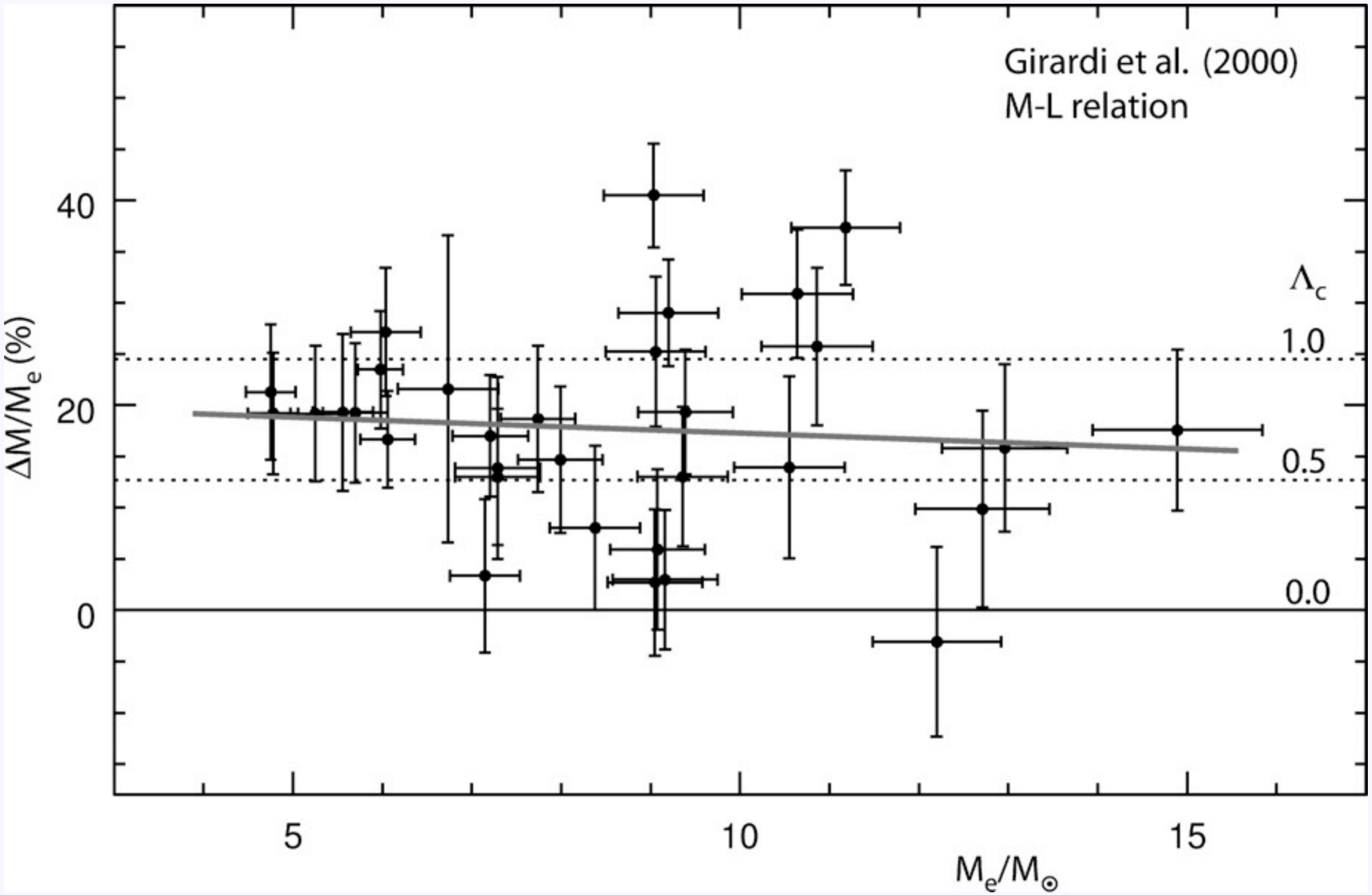

Mass offset when comparing masses from pulsation and from evolution for Cepheids (Keller 2008, ApJ 647, 483) showing an offset for pulsational minus evolutionary mass. Offset is explained here with convective core overshoot + mass loss ...

Motivation IV

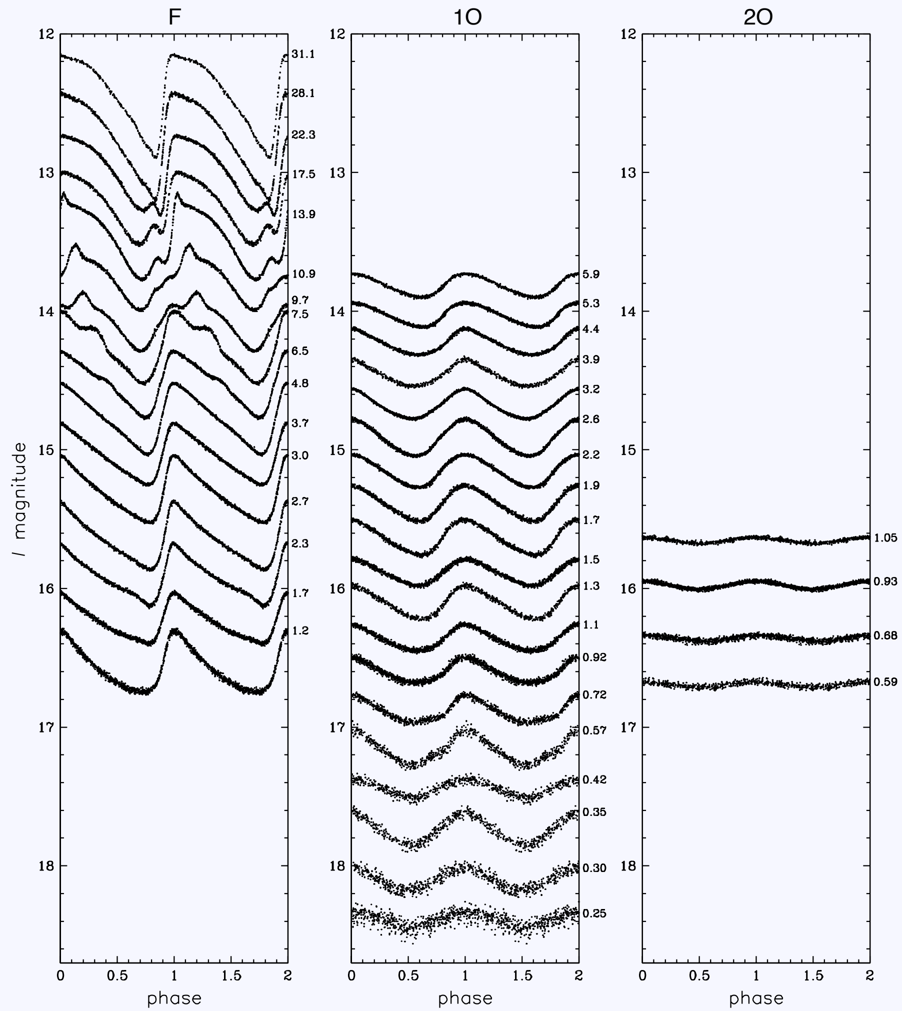

Fig. 1. Illustrative light curves of fundamental-mode (*left panel*), first-overtone (*middle panel*) and second-overtone (*right panel*) Cepheids. Small numbers at the right side of each panel show the rounded periods in days of the light curves presented in panels.

Lightcurves of Cepheids (from Soszyński et al. 2008, Acta Astron. 58, 163).

Motivation V

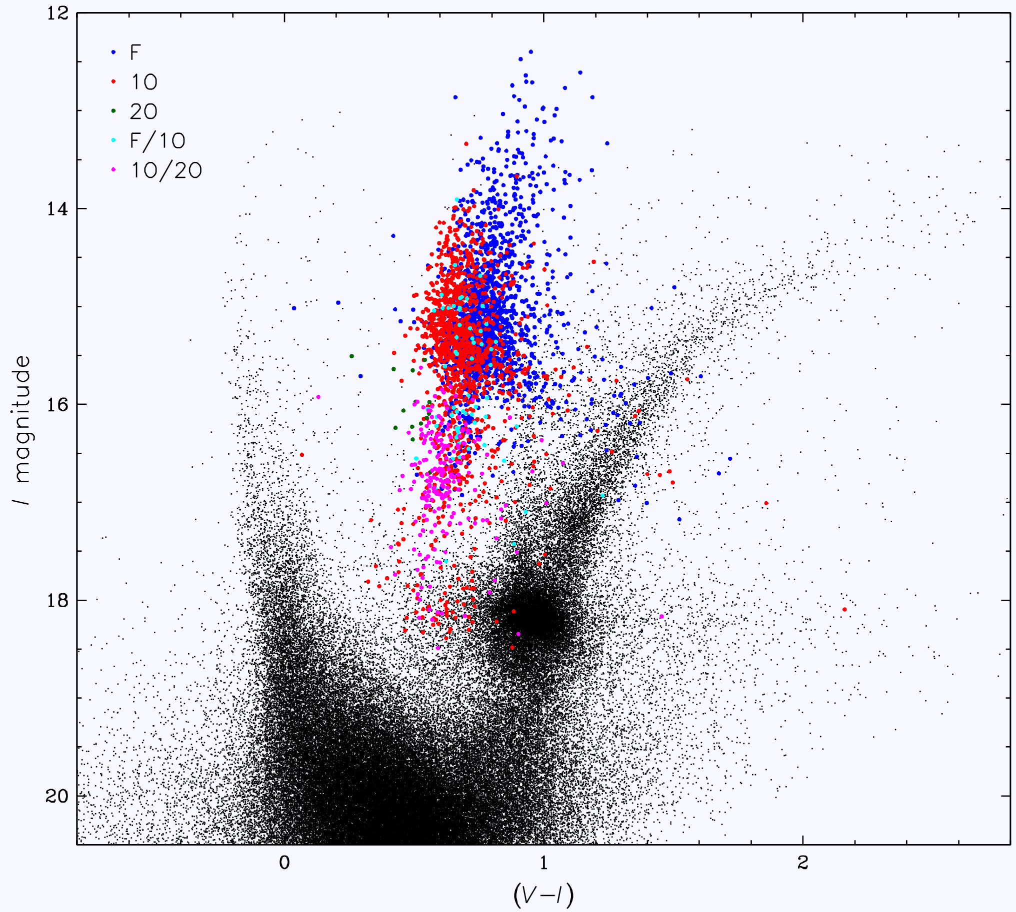

Fig. 7. Color–magnitude diagram for classical Cepheids in the LMC. In the background stars from the subfield LMC100.1 are shown. The significant number of very red Cepheids are clearly located to the red side of the respective instability strips for the various pulsation modes indicating that large reddening is not unusual in the LMC.

Observed distribution of various types of Cepheid pulsators in the LMC (from Soszyński et al. 2008, Acta Astron. 58, 163).

Motivation VI

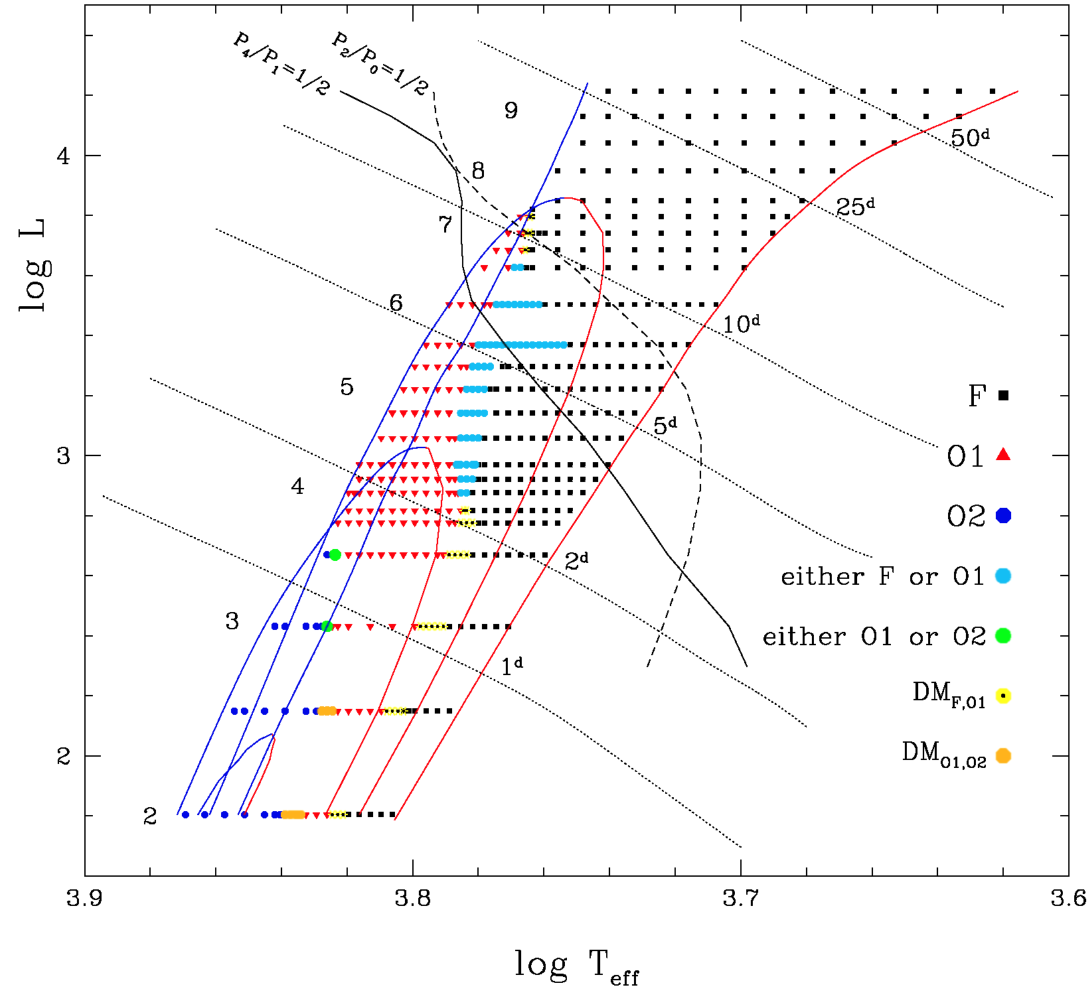

FIGURE 3. Computed HR diagram indicating the domains of single mode pulsations, of double mode pulsations and of hysteresis

Theoretical location of double-mode Cepheids (from Buchler 2009, APC 1170, 61).

Motivation VII

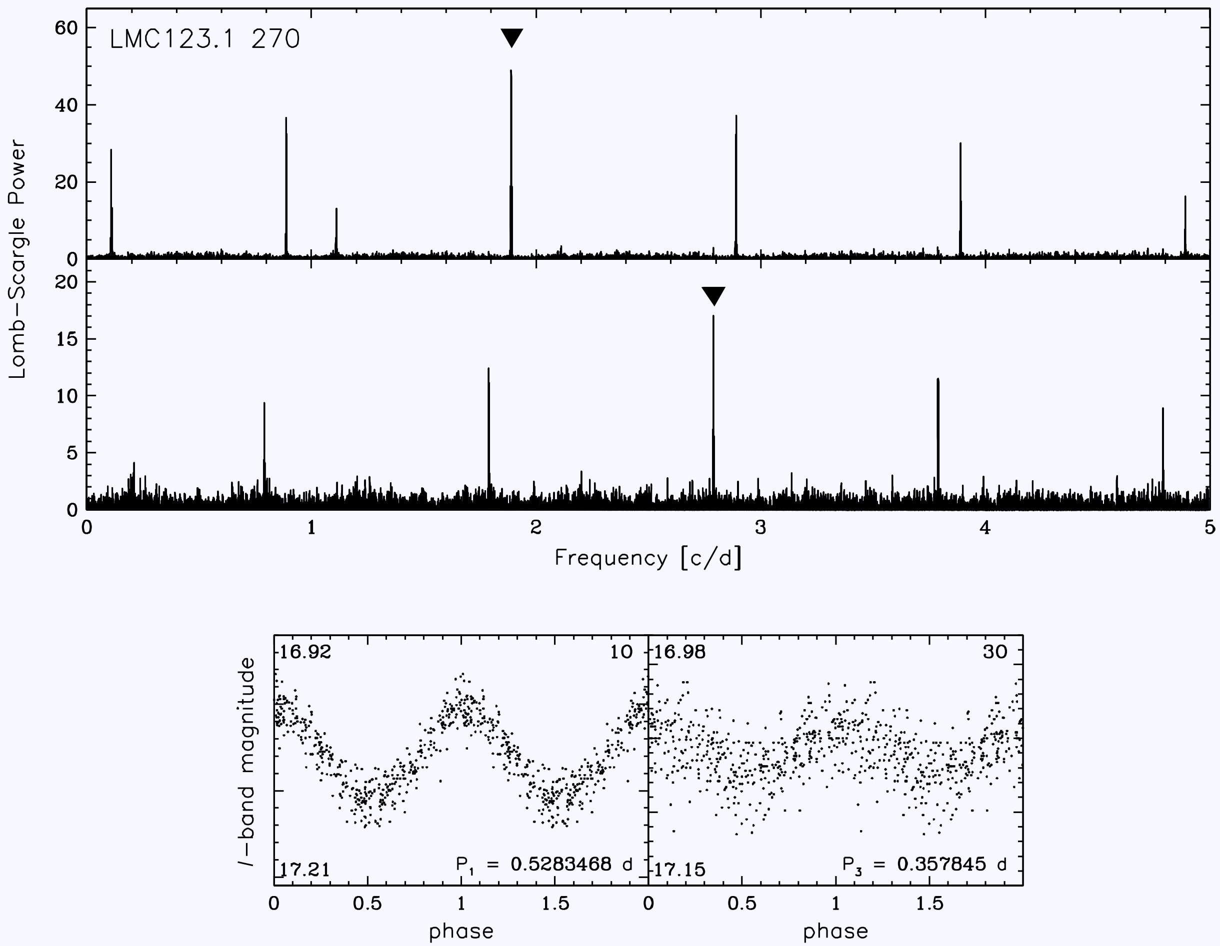

Fig. 4. Power spectra and light curves of 1O/3O double-mode Cepheid LMC123.1 270. Two *upper panels* show power spectra for the original data and after subtracting the primary periodicity, respectively. *Bottom panels* display light curves folded with the primary and secondary periodicities after prewhitening with the other period.

Identifying double-mode pulsators (from Soszyński et al. 2008, Acta Astron. 58, 153).

Motivation VIII

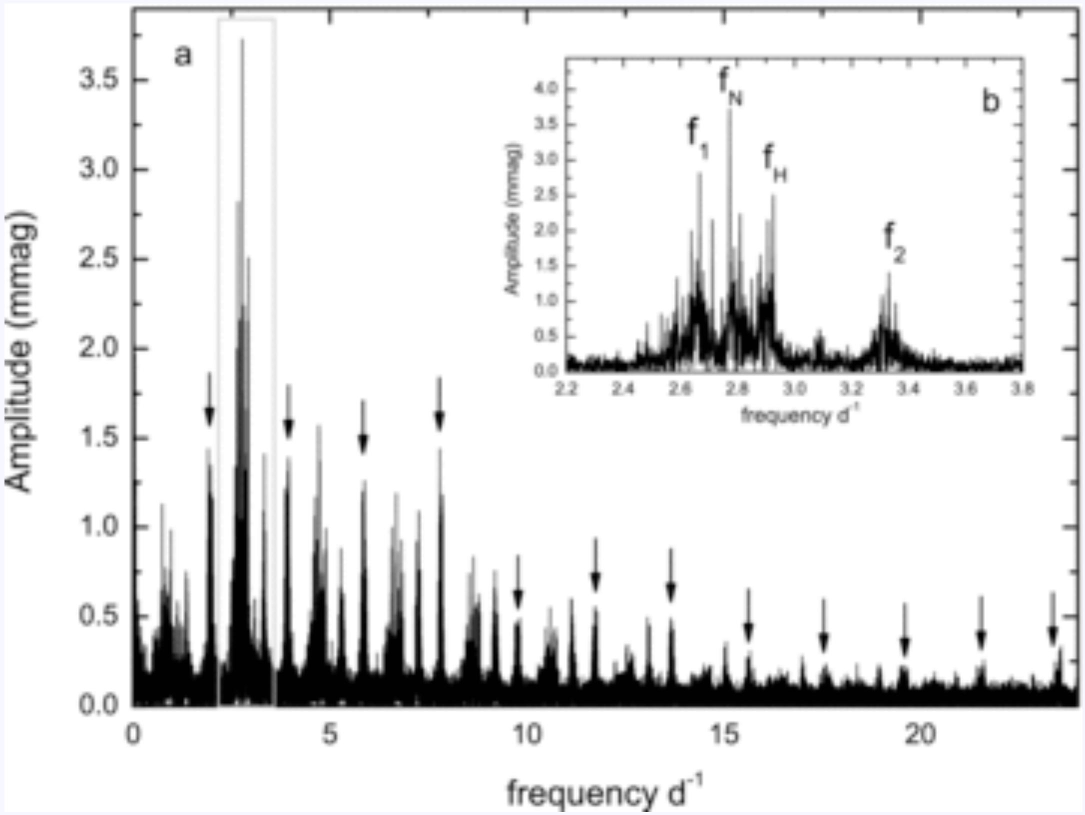

Table 6. Comparison of the overtone modes and the additional frequency of the two stars.

	CoRoT 105288363	V445 Lyr
f_2 (d^{-1})	2.9856	3.3307
$A(f_2)$ (mmag)	0.5	1.4
f_0/f_2	0.590	0.585
f_1 (d^{-1})	2.3793	2.6676
$A(f_1)$ (mmag)	0.3	2.7
f_0/f_1	0.741	0.731
f_N (d^{-1})	2.442	2.7719
$A(f_N)$ (mmag)	0.4	3.6
f_0/f_N	0.722	0.703

Identifying a non-radial mode (f_N) in classical variables (RR Lyr stars in the case), in this case V445 Lyr (from Guggenberger et al. 2012, MNRAS 424, 649).

Motivation IX

“Stationary” line profiles of A-, F-type supergiants

Observations (black, solid line) vs. standard 1D models with microturbulence (red, dashed line) of a rather strong and a rather weak spectral line. T_{eff} sequence from 9250 K to 6500 K. Left panel: Ti II, 4563.76 Å. Right panel: Cr II, 4554.99 Å.

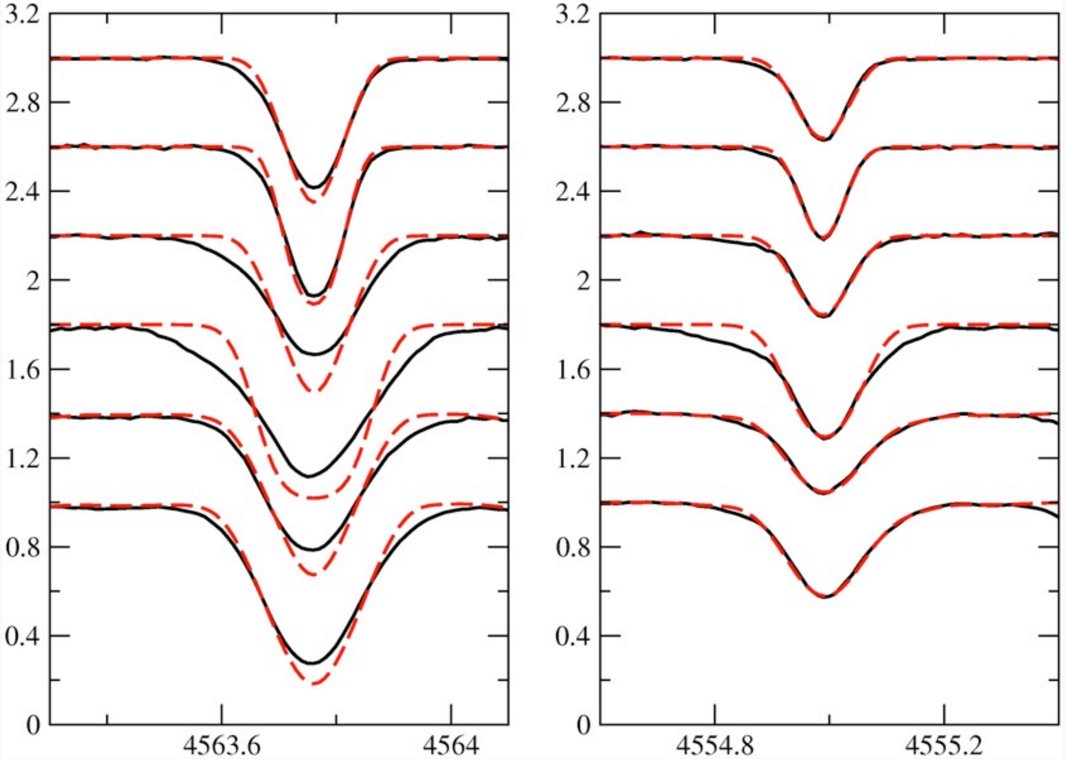

Objects: HD 46300 (13 Mon), HD 87737 (η Leo), HD 175687 (ξ^1 Sgr), HD 147084 (o Sco), HD 182835 (ν Aql)

Spectral types: A0 Ib, A0 Ib, A0 II, A4 II-III, F2 Iab

T_{eff} : 9700 K, 9700 K, 9400 K, 7850 K, 6800 K

from Landstreet et al. 2009, A&A 503, 973

Motivation X

Time dependent line profiles of Cepheid X Sgr

Evolution of the Fe I 6056 Å line profile in X Sgr (pulsation phase 0.968 to 2.537). Gaussian fits for different components and their evolution are symbolised by a given colour. Rest wavelength indicated by a red, vertical line (Fig. 1 from Mathias et al. 2006, A&A 457, 575. Fig. 4 shows the same phase variation for Hα).

Observations are interpreted here as the result of two shock waves crossing the photosphere in each pulsation phase.

Unusually strong for Cepheids. Correct ?

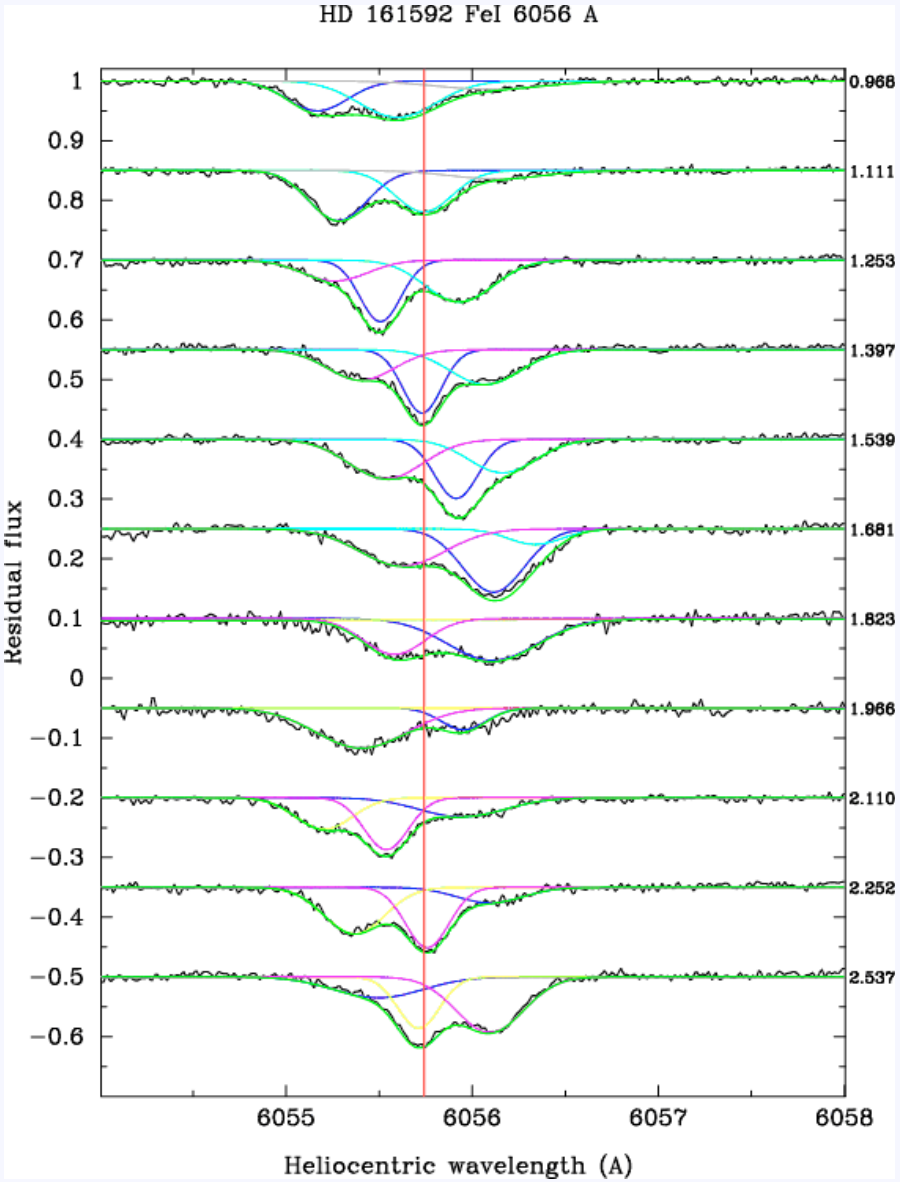

Motivation X

Time dependent line profiles of Cepheid X Sgr

Evolution of the Fe I 6056 Å line profile in X Sgr (pulsation phase 0.968 to 2.537). Gaussian fits for different components and their evolution are symbolised by a given colour. Rest wavelength indicated by a red, vertical line (Fig. 1 from Mathias et al. 2006, A&A 457, 575. Fig. 4 shows the same phase variation for Hα).

Observations are interpreted here as the result of two shock waves crossing the photosphere in each pulsation phase.

Unusually strong for Cepheids. Correct ?

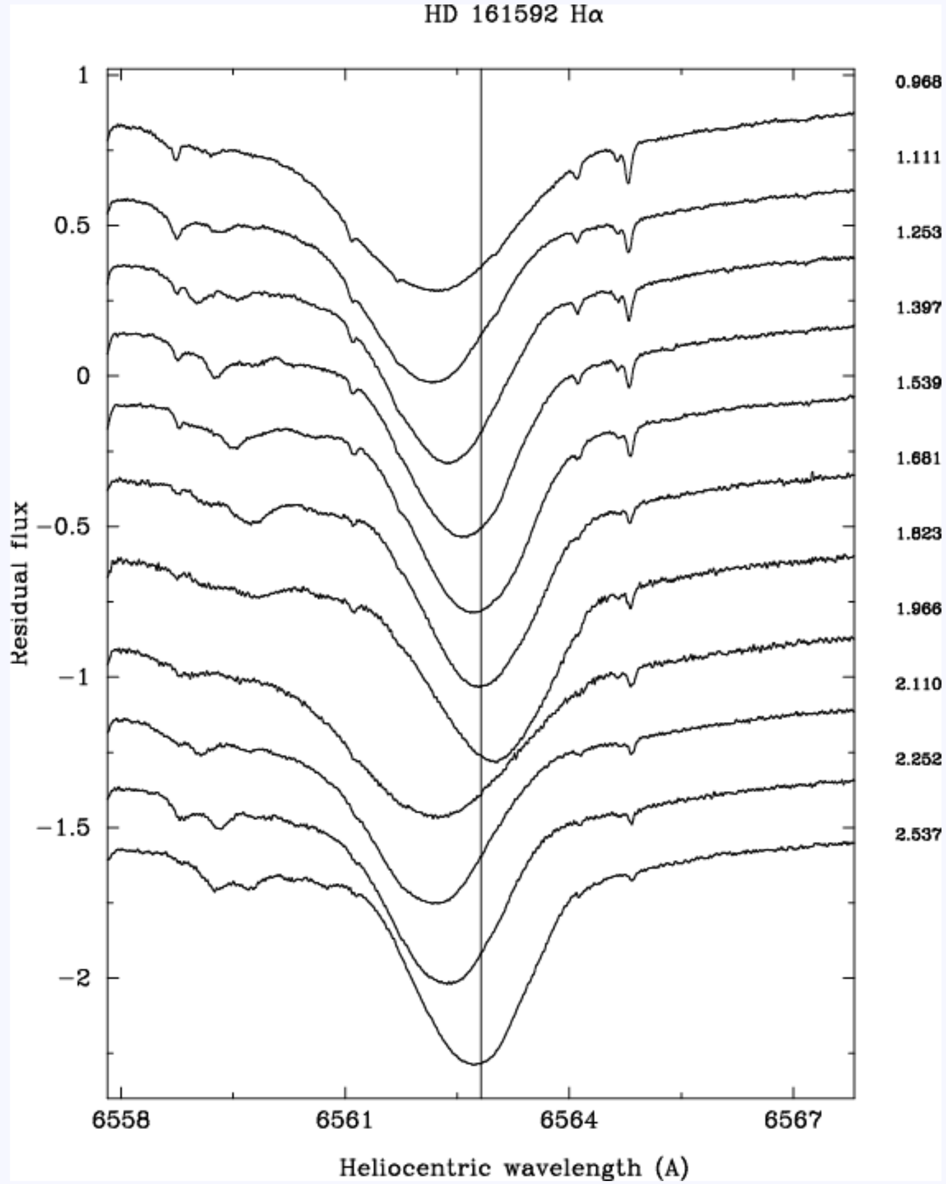

Motivation XI

Challenges to previous modelling

- 1D pulsation (and also evolution) models rely on
  - variants of non-local MLT
  - up to 8 free parameters (Buchler & Kolláth 2000, NYASA 898, 39)
  - parameters that are calibrated (?) or guessed
  - while values determine the model predictions (!), for instance,
  - the location of red edge of the instability strip of Cepheids is determined by turbulent pressure
- Parameter determination with spectroscopy
  - Anaylses mostly assume static, homogeneous atmospheres,
  - but does this at least approximately hold ?

→ ***numerical hydrodynamical simulations in 2D and 3D***

The ANTARES Code I

The ANTARES code

(ANTARES — A Numerical Tool for Astrophysical RESearch)

- general purpose Fortran95 code for hydrodynamical simulations
- development initiated by H.J. Muthsam
- main development site: Faculty of Mathematics at Univ. of Vienna, formerly also at MPA in Garching, and now also at
- BTU Cottbus (Germany), Lab. d'Astrophys. Toulouse (France)
- presently only available to developers and direct collaborators
- currently ~150000 lines of code in active modules
- modular, fully MPI parallelized code (+ OpenMP for load balance)
- post-processing with Paraview and statistics programs

The ANTARES Code II

Equation types and problem classes

- time dependent hydrodynamics: in 1D, 2D, and 3D
- single or two-component fluid model
- stationary, LTE 3D (+ short characteristics) radiative transfer
- optionally: MHD equations
- either equidistant Cartesian grid or
- polar grid, radial component co-moving with mean velocity

Microphysics

- realistic EOS, opacities: OPAL, LLNL, ATLAS9 / Kurucz
- or idealised microphysics (prescribed heat conductivity, constant ratios of other diffusivities, perfect gas)
- or EOS and conductivities for saltwater (→ oceanography)

The ANTARES Code III

Numerics

- conservative, high resolution advection with WENO5
  - 5th order weighted essentially non-oscillatory method (optimizes numerical viscosity, allows for iLES type simulations)
- discretization of parabolic terms consistent with ENO methods
- vertically closed or open boundaries, horizontally periodic
- time evolution from perturbed 1D or 2D equilibrium states
- optional: grid refinement
- optional: subgrid scale models (→ unresolved scales) in addition to iLES (implicit Large Eddy Simulation) approach
- new time integration methods (operator splitting, for low Mach numbers and fast radiative cooling, partially “in-house made”)

The Numerical Challenges I

The Cepheid we model...

- Its basic stellar and simulation parameters are:
  - T_{eff} = 5125 K, log(g) ~ 1.97, M = 5 $M_\odot$, R ~ 38.5 $R_\odot$, L ~ 913 $L_\odot$, X = 0.7, Y = 0.29, Z = 0.01, P = 3.85 d, first overtone (1O)
  - outer 42% of R, vertical grid spacing: 0.47 Mm ... 124 Mm (modelling only the outer 42% → implies P somewhat too short)
- computational concept
  - idea: simulate flow in a wedge with fixed opening angle
  - boundaries: vertically closed (recent: open top), azimuthally open
  - an integer multiple of such wedges constitutes a ring in the equatorial plane (→ independent of polar angle: 2D simulation)
  - gravitational stratification → how to resolve stellar boundary ?
    → Radially stretched grid co-moving with mean radial velocity !

The Numerical Challenges II

Grid and geometry parameters

- opening angles, grid refinement, and stretching factors:
  - 1° opening angle, 800 × 300 points ➔ resolves H ionization zone
  - 10° opening angle, 510 × 800 points ➔ study He II ionization zone
  - model with 3° opening angle and grid refinement to combine both

  ➔ selection of models from Mundprecht et al. (2013)

  (submitted to MNRAS, preprint at arXiv:1209.2952)

model nr.	aperture angle	grid points radial	grid points polar	stretching factor	subgrid modelling	grid refinement	radial cell size	refined radial cell size
1	10°	510	800	1.011	no	no	0.47 . . . 124 Mm	
2	3°	510	300	1.011	yes	no	0.47 . . . 124 Mm	
3	3°	510	300	1.011	yes	yes	0.47 . . . 124 Mm	0.32 . . . 0.80 Mm
4	1°	800	300	1.007	yes	no	0.29 . . . 79 Mm	

Table 1. Grid parameters for the different numerical Cepheid models discussed in this paper.

The Numerical Challenges III

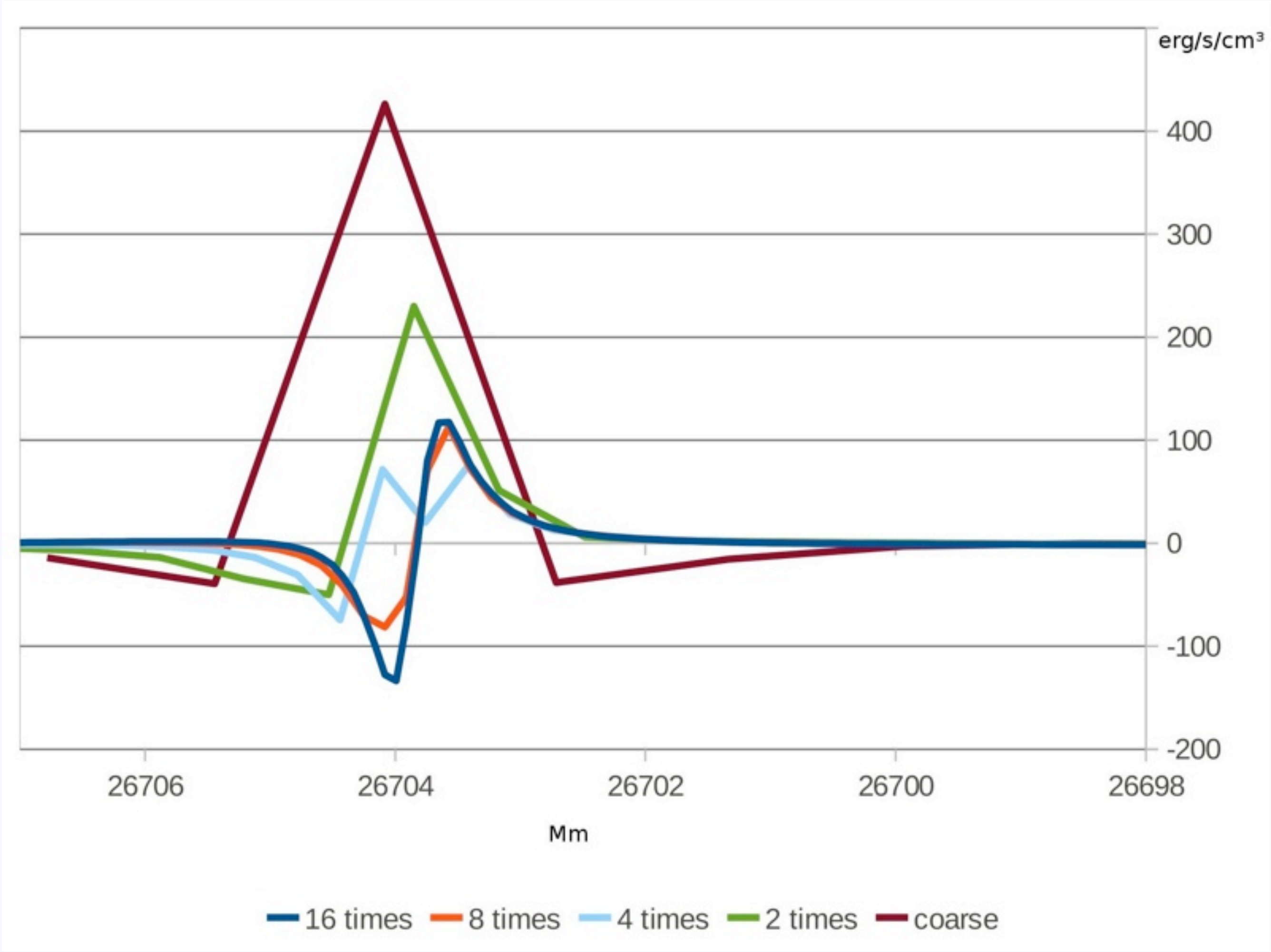

Resolution and time stepping: Q_{rad} in the H I ionization zone from 1D models of various resolutions (vertical refinement: different colours). From Mundprecht et al. (2013).

The Numerical Challenges IV

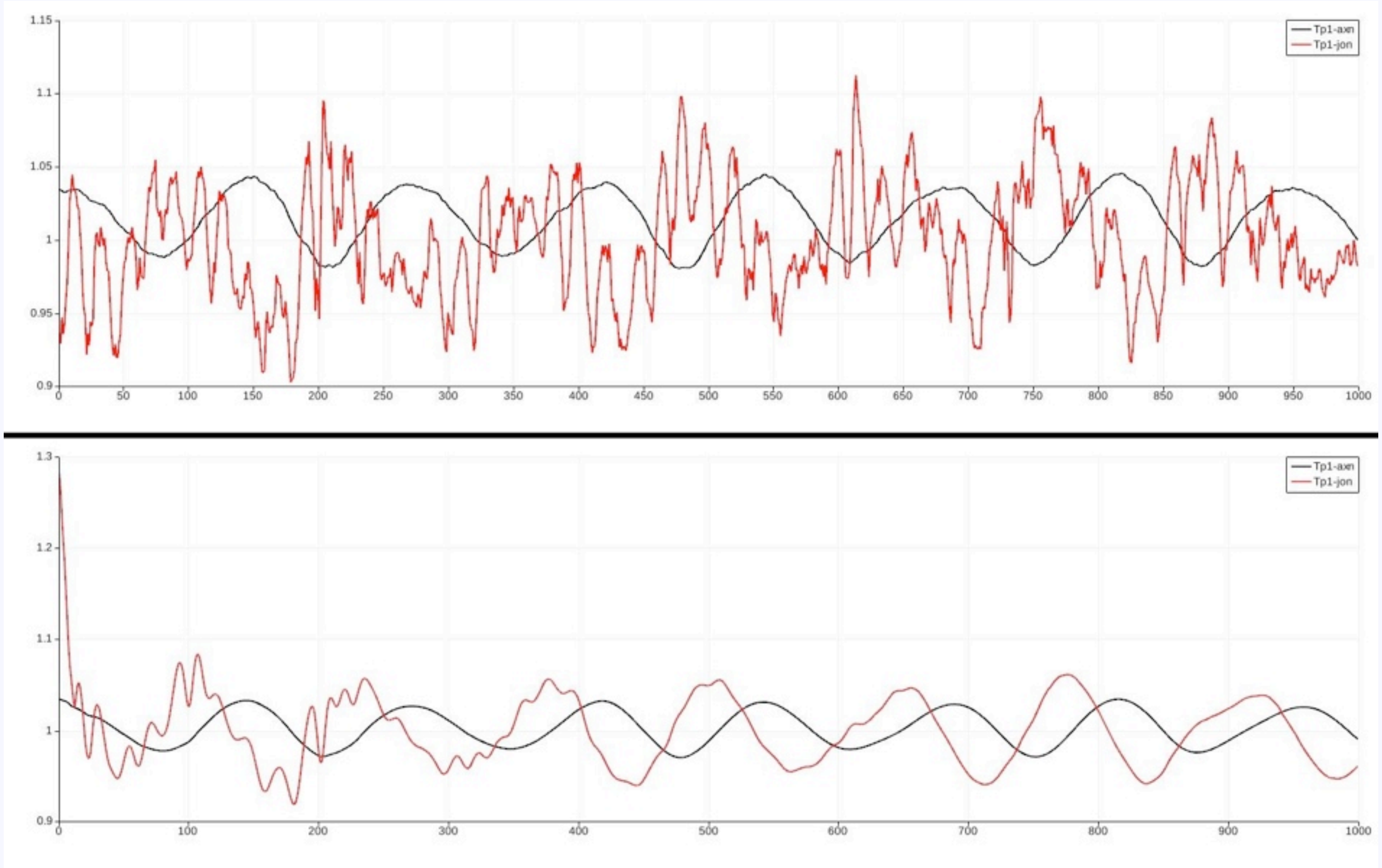

1D model lightcurve (red), runnig mean (black), 8 pulsation periods (1000 output steps). Lower panel: results at 4x higher resolution. Note the 30% drop (Mundprecht et al. 2013).

The Numerical Challenges V

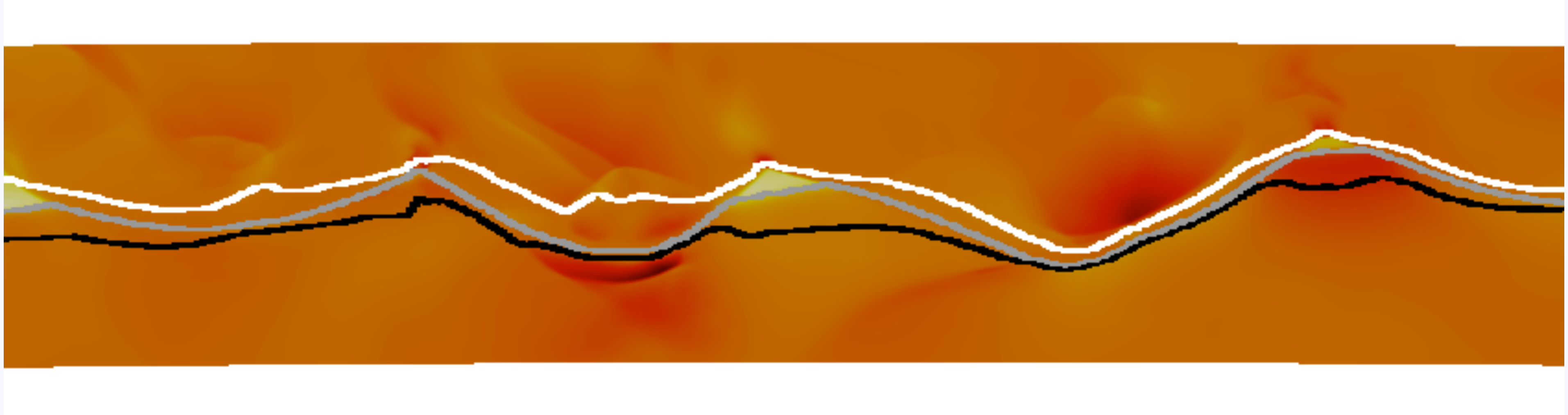

Convective flux (colours) and optical depth (three isolines at τ = 1, white, 10, grey, and 100, black) in a high resolution model, 1° of width shown (from Mundprecht et al. 2013).

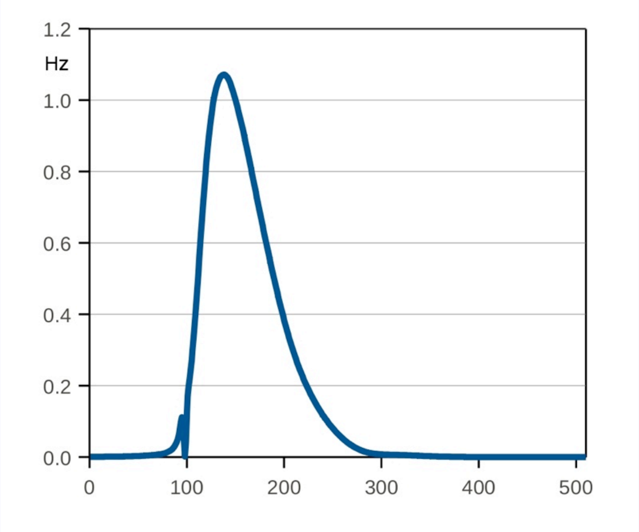

Reciprocal radiative time scale times the Courant number, as a function of depth, at moderate resolution (from Mundprecht et al. 2013).

→ solve resolution problem with an adaptive grid, adjusted to ease time step constraints

The Numerical Challenges VI

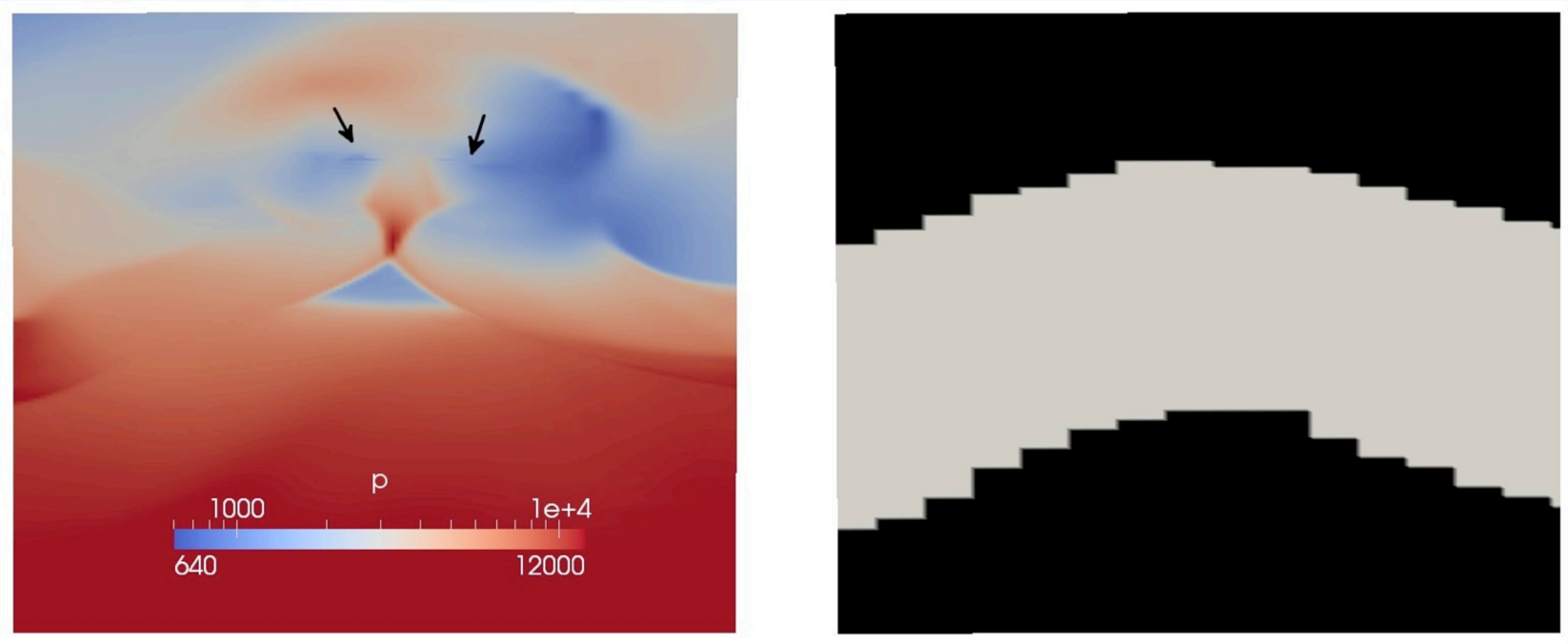

Lower boundary chosen to avoid very small time steps due to radiative diffusion. Artifacts (horizontal lines) in the pressure field (CGS units used), if the grid refinement zone has an upper boundary in the photosphere (from Mundprecht et al. 2013).

The Numerical Challenges VII

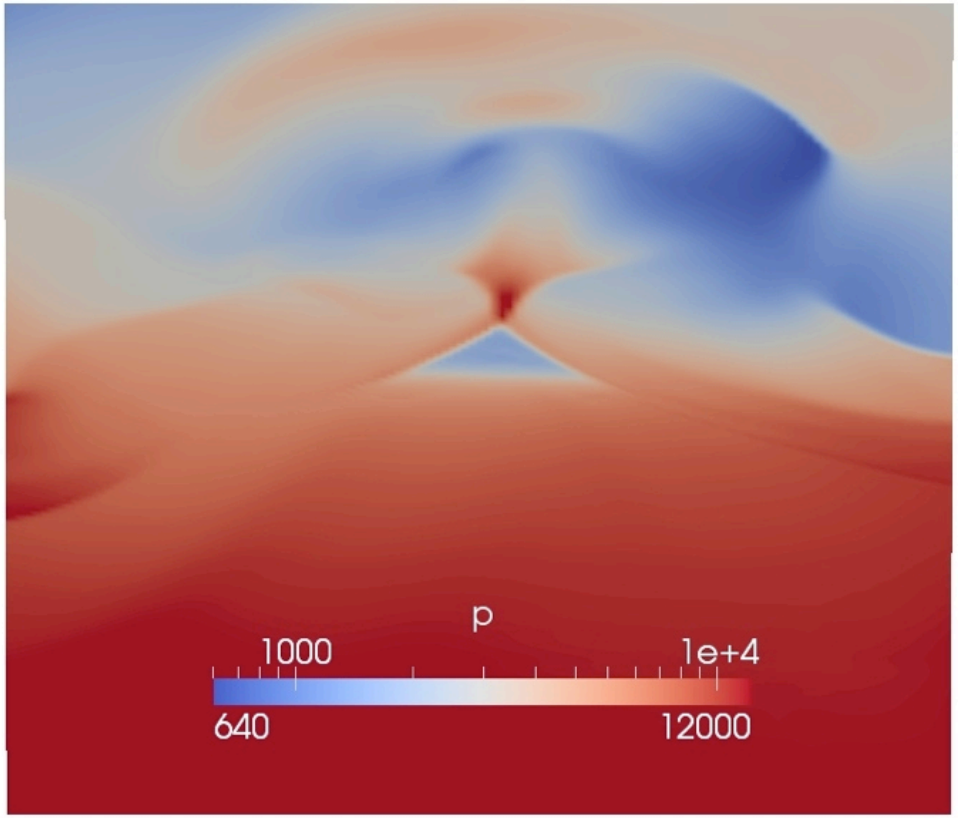

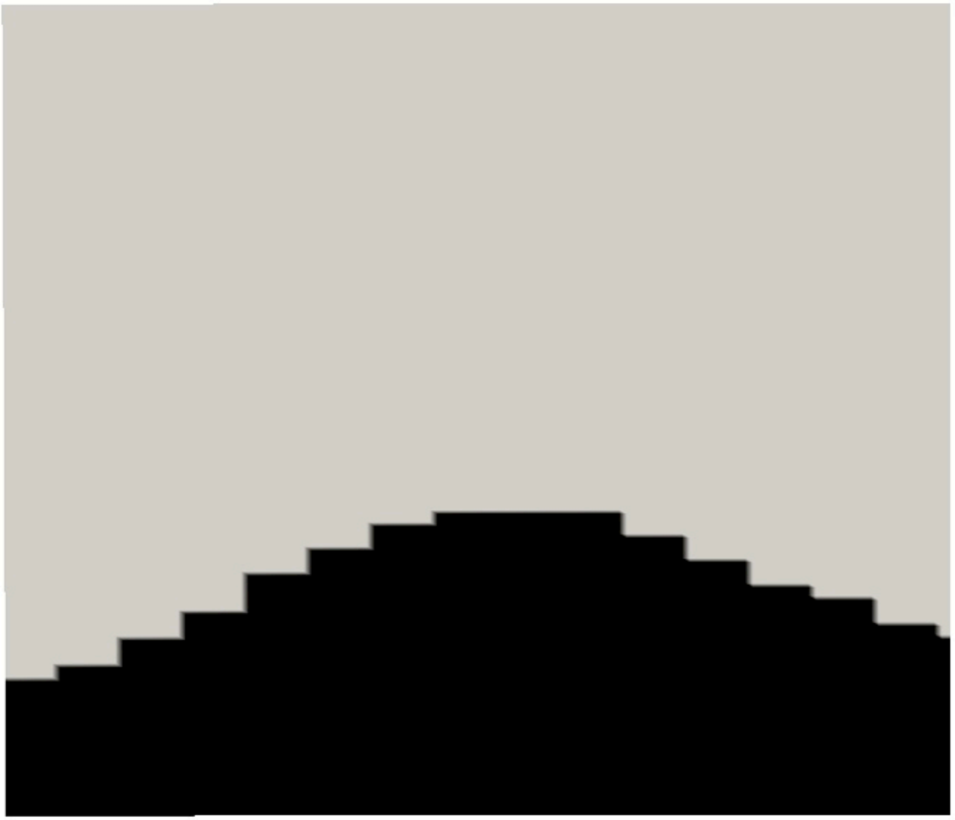

These artifacts are removed, if the grid refinement zone extends all the way up to the top of the simulation domain. The lower boundary of the refinement zone, located in the region of radiative diffusion, does not cause further artifacts (from Mundprecht et al. 2013).

The Numerical Challenges VIII

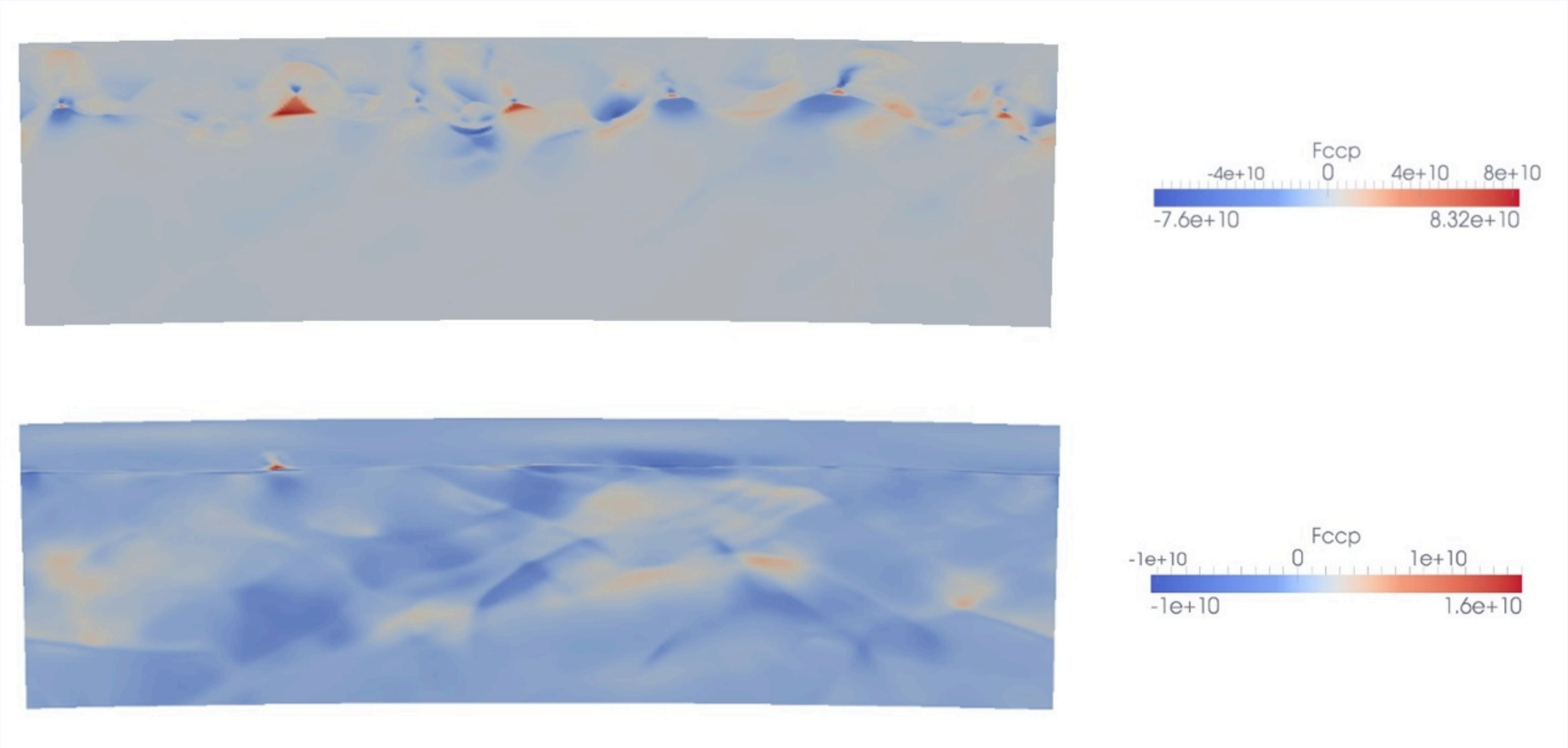

Convection in the H I ionization zone. Upper panel: model 3 with grid refinement (by 3 × 4), lower panel: model 2, without grid refinement. Note the change in scale for F_{conv} and the change in the flow patterns observed in the overshooting zone (from Mundprecht et al. 2013).

Simulation Results I

Goals of the study

- high resolution models: the 1° model
  - development of the H I ionization zone
  - dynamics of the photosphere
- large opening angle: the 10° model
  - development of convection in the He II ionization zone
  - phase shifts & interaction between convection and pulsation ?
  - probe recipies for F_{conv}, i.e. detemine one of model parameters of the Kuhfuß and Stellingwerf models
  - compute work integrals as a function of phase

Simulation Results II

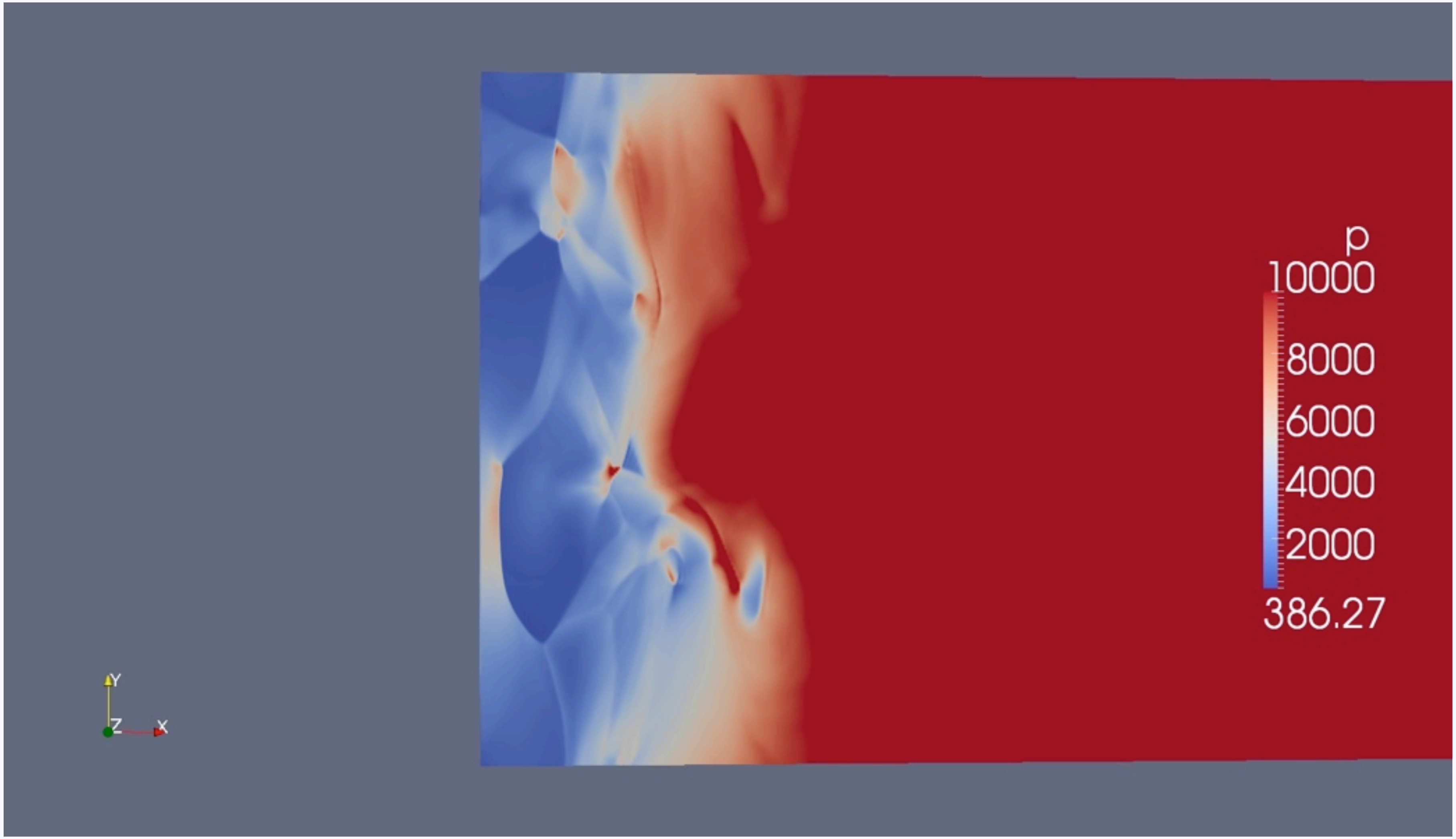

Development of shock fronts in the photosphere for the 1° simulation (pressure: CGS units). Mach numbers are up to 4 in this case (cf. Muthsam et al. 2013, in prep.).

Simulation Results III

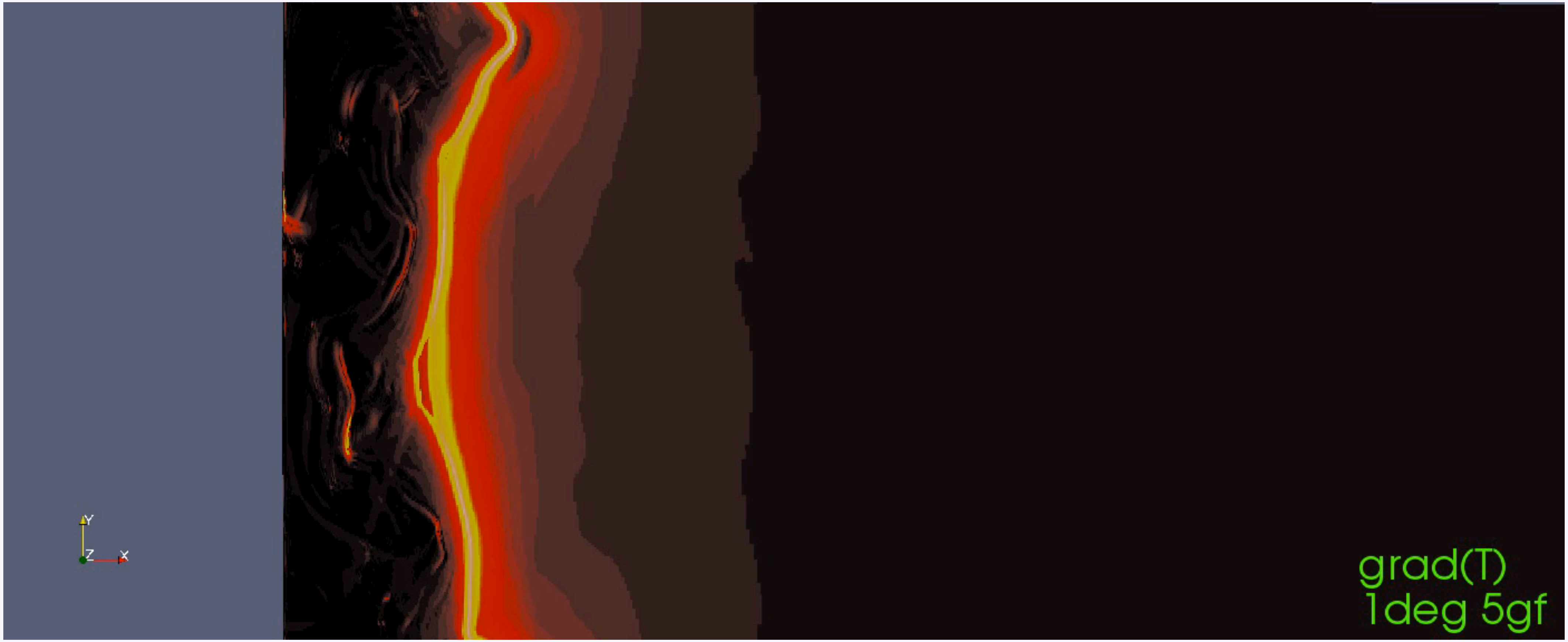

Development of the temperature gradient in the 1° simulation during the contraction phase of the pulsation cycle (see also (Muthsam et al. 2013, in prep.).

Simulation Results IV

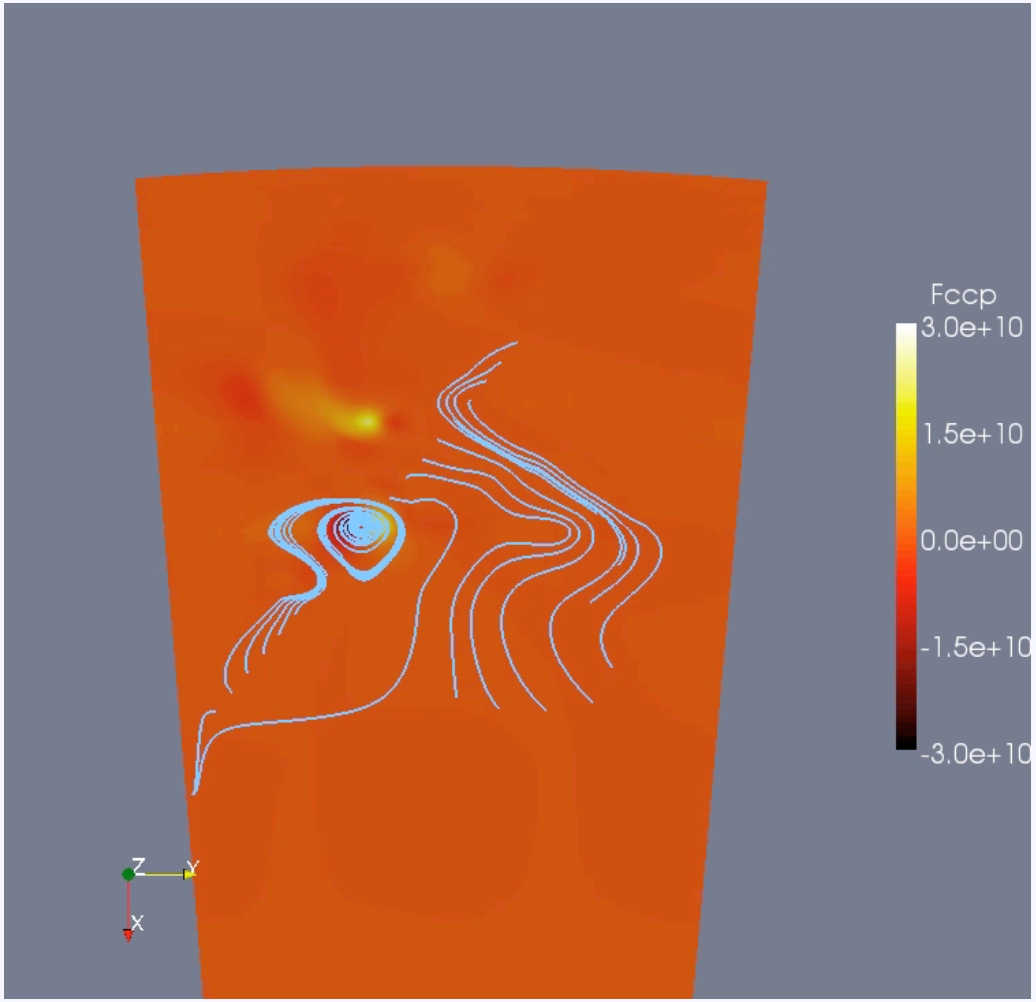

F_{conv} and selected velocity stream lines in the He II ionization zone for the 10° model over one pulsation cycle (Mundprecht, PhD thesis, 2011; Muthsam et al. 2011, IAU S 271, 179).

Simulation Results V

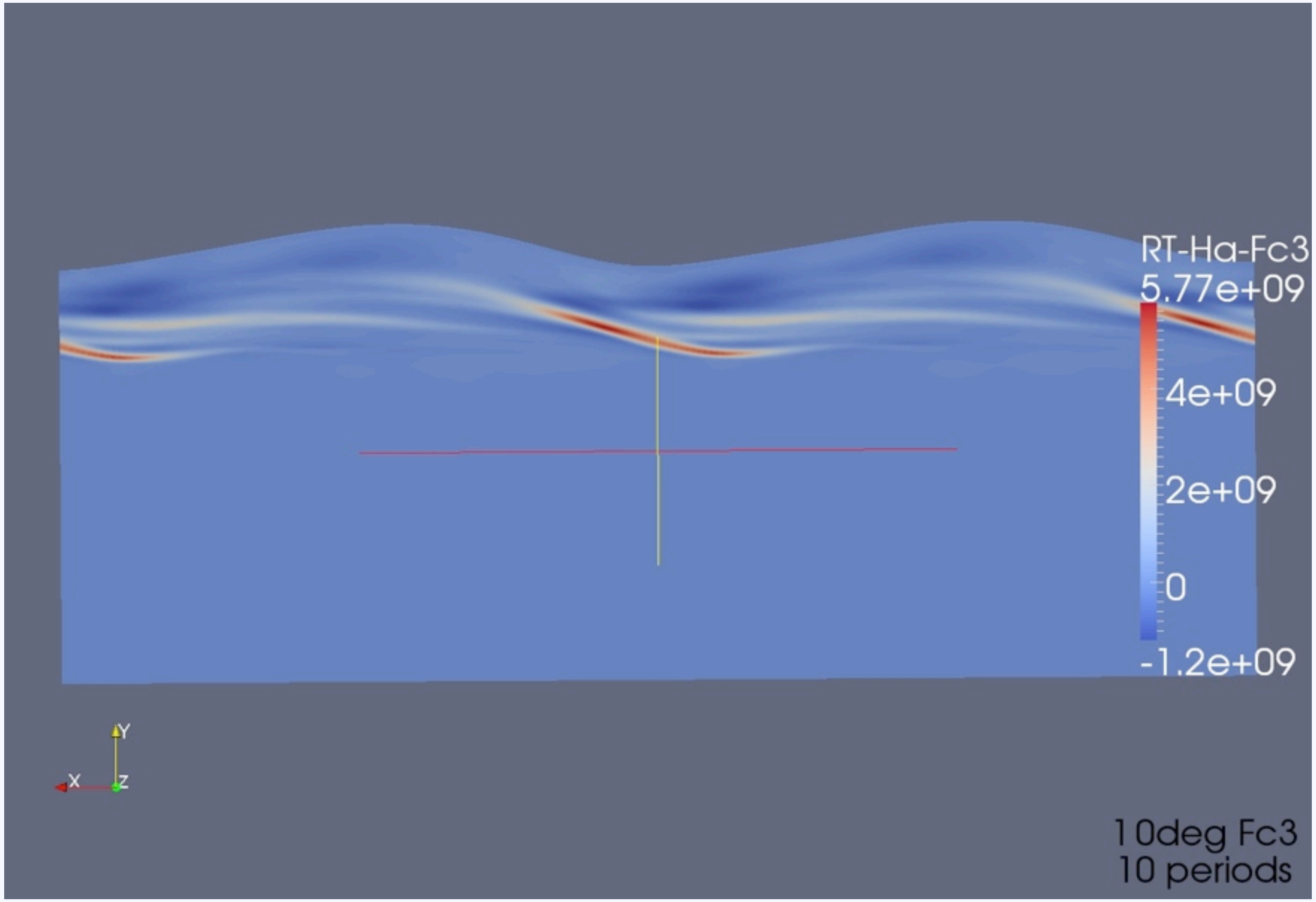

F_{conv} in the 10° simulation. Radial dependence as a function of phase. The phase average over 10 periods is displayed twice. Note the variation within the region of He II ionization. From Muthsam et al. (2013, in prep.).

Simulation Results VI

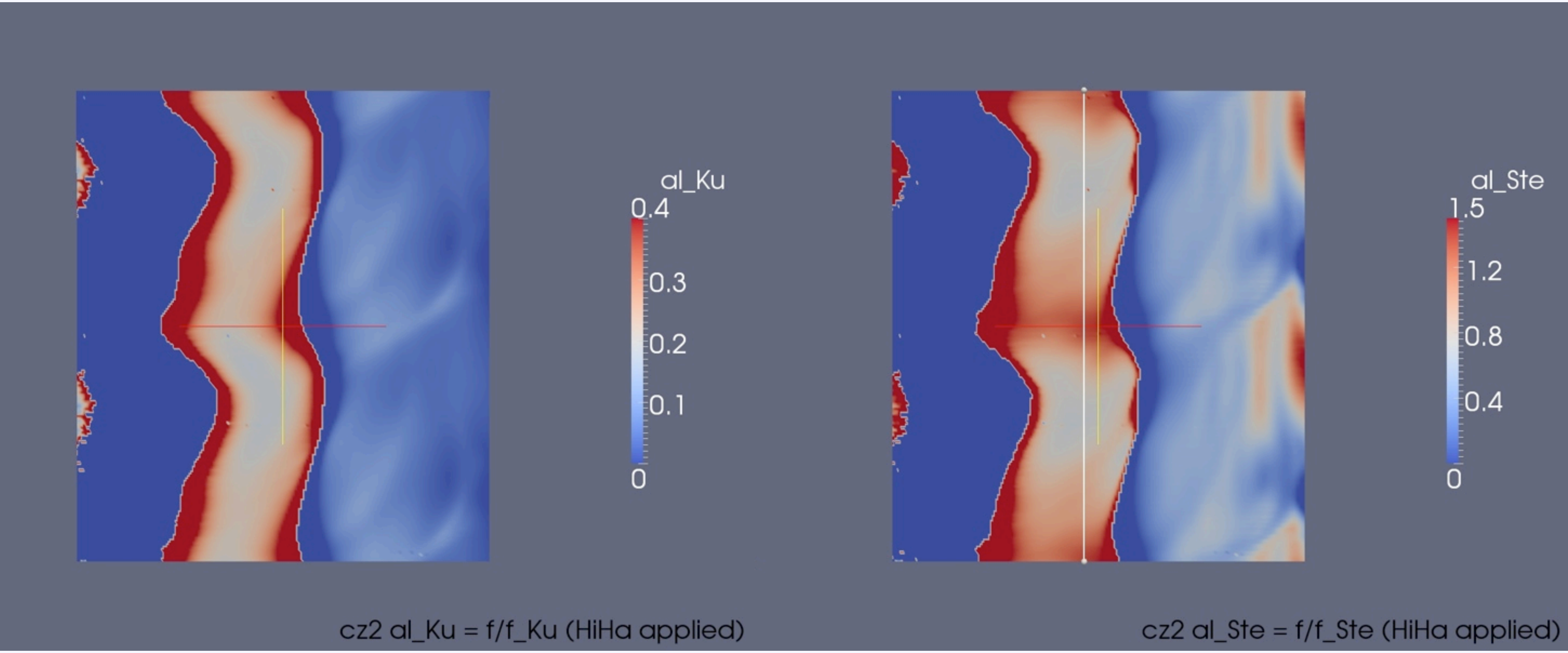

F_{conv} in the 10° simulation within and around the region of He II ionization: optimum parameter α_c averaged horizontally for each phase (plotted twice) and shown as a function of depth. Left panel: Kuhfuß model, right panel: Stellingwerf model (from Muthsam et al. 2013, in prep.).

Simulation Results VII

TDC	variant		convection zone			overshooting region		
	designation	α_{r}	α_{c}	σ	$\frac{\alpha_{\max}}{\alpha_{\min}}$	α_{c}	σ	$\frac{\alpha_{\max}}{\alpha_{\min}}$
KF	Pr_trb1	0.30	10.77	29.4	2.8	1.58	9.1	1.4
	Pr_trb2	0.30	7.20	21.6	2.2	0.93	13.0	1.6
	Ps_trb1	0.08	3.15	28.4	2.6	0.45	9.4	1.4
	Ps_trb2	0.08	2.07	20.7	2.1	0.27	13.3	1.7
SW	Pa_trb1	0.10	1.12	25.1	2.2	0.47	7.4	1.3
	Pa_trb2	0.10	0.73	14.3	1.6	0.26	9.9	1.4
	Pb_trb1	0.25	1.33	27.3	2.3	0.56	8.4	1.3
	Pb_trb2	0.25	0.84	15.4	1.6	0.29	10.0	1.4

Table 1. α-values for various convection models: the designation indicates whether the x-component only is used for evaluating turbulent kinetic energy (trb1) or whether also the y-component is used (trb2). The letters r, s, a, and b in Pr, Ps, etc. refer to the value of α_{r} adopted (listed in the next column). α_{c} is the mean value, σ the standard deviation in percent of the mean value (averaged each over ten periods). The ratio $\alpha_{\max}/\alpha_{\min}$ is a measure for the total amplitude of the variation of α_{c} over one period.

Parameter α_c for the convective flux in the Kuhfuß and Stellingwerf models and the 10° simulation within and around the region of He II ionization (from Muthsam et al. 2013, in prep.).

Simulation Results VIII

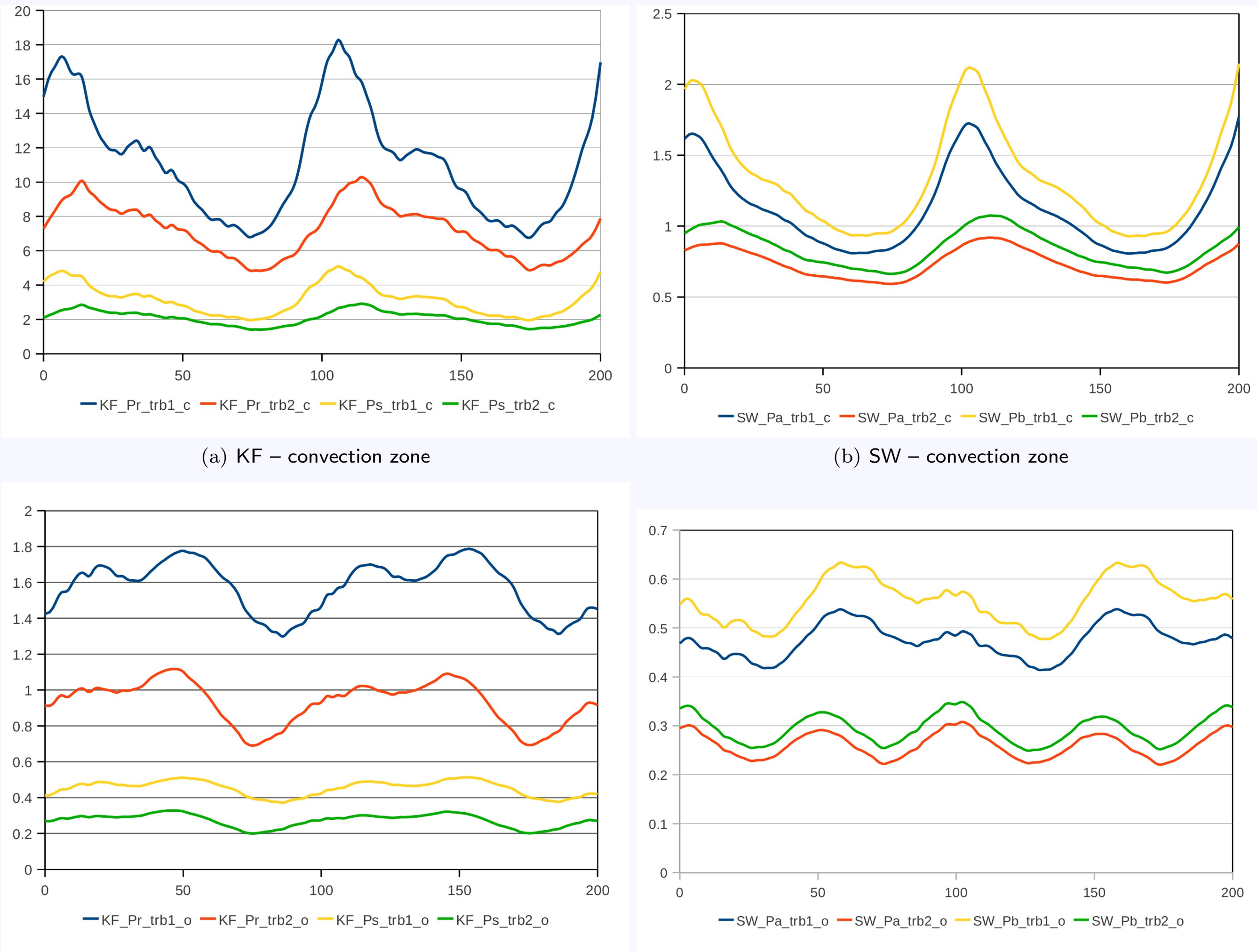

(a) KF – convection zone

(b) SW – convection zone

(c) KF – overshooting region

(d) SW – overshooting region

Figure 3. The parameter α_c as a function of time: horizontal averages over $\sim$2 periods (a value of 200 corresponds to two full periods). In the different panels KF denotes results from testing the Kuhfuß model and SW results from testing the Stellingwerf model. Letters r, s, a, and b after P in the designation identify different values of α_r. The results denoted by trb1 include only the vertical velocity in the computation of the turbulent energy while for results denoted by trb2 the horizontal velocity was included as well. The letters c and o refer to the convection and overshoot regions, respectively.

Analyzing the 10° simulation within and around the region of He II ionization.

Variation of optimized α_c parameter for the convective flux in the Kuhfuß and Stellingwerf models shown for two periods (from Muthsam et al. 2013, in prep.).

Simulation Results IX

Main Conclusions

- high resolution: the 1° model
  - once there is sufficient resolution, convection develops in the H I ionization zone
  - occurrence of strong shock fronts and other phenomena in the photosphere
  - open vertical boundary condition on top required (for more stable integration)
  - may result in a net outflow
- wide opening angle: the 10° model
  - increase in convective driving in the He II zone during contraction
  - a phase lag exists between radius and extent of the convection zone (static picture of convective layers fails)
  - neither the Stellingwerf nor the Kuhfuß model recover F_{conv} over a period with fixed model parameters
  - variation of α_c over phase and as function of r evident (factors of 2 to 10)
  - improved models must account for Pe-dependence, enhanced TKE (turbulent kinetic energy) dissipation in overshoot region, anisotropy of TKE, among others

Recent Work and Outlook I

What can be done, if...

- you just use 277 points radially instead of 510,
- but 13000 points azimuthally instead of 800 ? And
- have (several) 500,000 CPU-core hours at your disposal ?

... among others, you might have a look at

- excitation of non-radial modes
- investigate the natural azimuthal width of flow structures

As a teaser:

- How about the first 14 pulsation cycles of a 360° model ?
- And otherwise the same parameters as for the 10° model ?

Recent Work and Outlook II

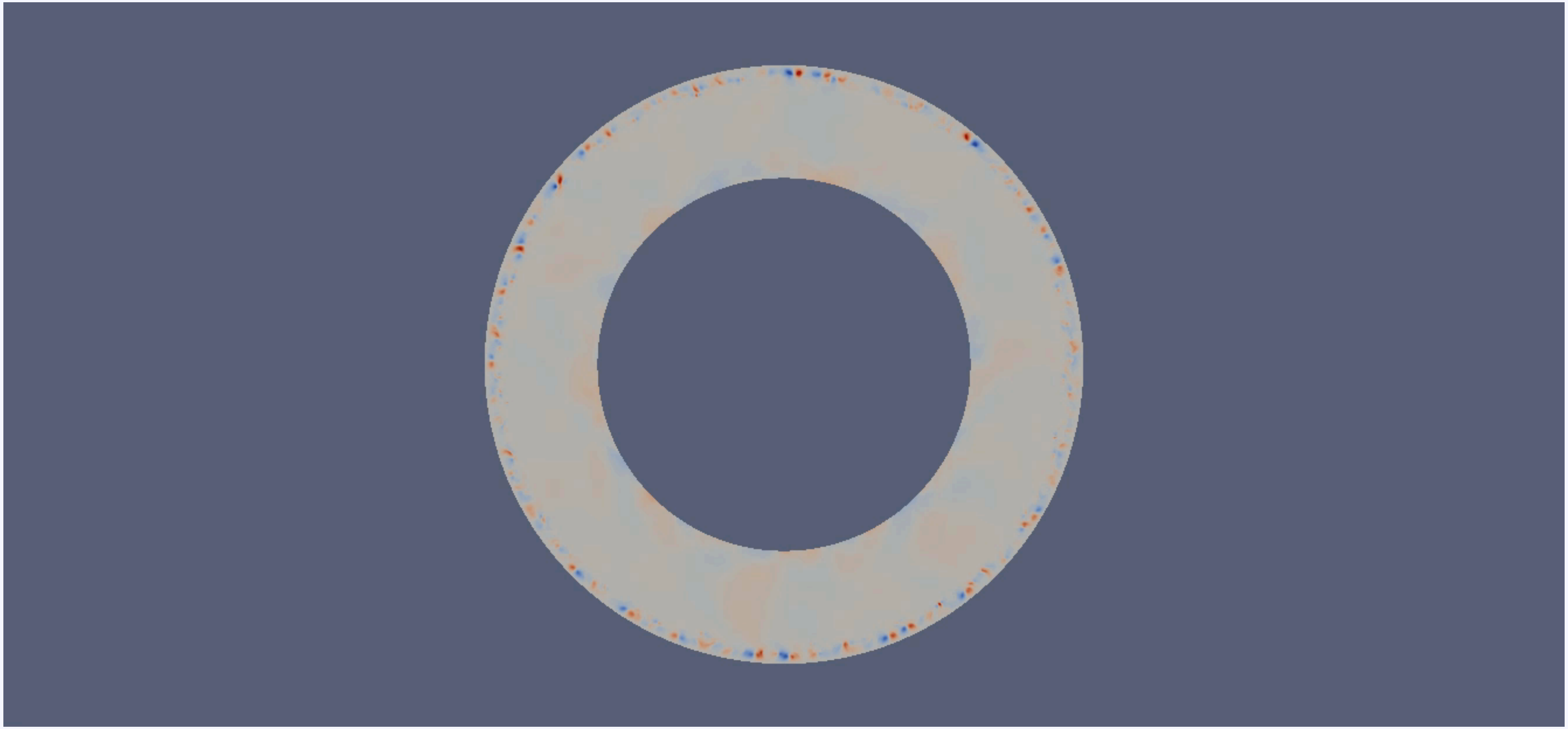

Simulation of the time development of a Cepheid. Simulation box: the full equatorial plane. Colour: vertical momentum density. The first 14 pulsation cycles are shown.

Recent Work and Outlook III

Some ongoing work

- boundary conditions
  - upper open boundary conditions (stable longterm runs of high resolution models): implemented, currently being tested
- implicit time integration
  - to further ease the restrictions due to radiative diffusion
    - faster computation, longer time series
  - done for the 1D, almost finished for the 2D case, required development of a parallelized, non-linear multigrid solver
- extended simulations with 360° models
- longterm goals: a 3D simulation for the same scenario
  (would be much easier for idealized microphysics which would not yield realistic models, the very goal of the present work)

...THANK YOU FOR YOUR TIME !